

Joint IQ Imbalance Compensation and Channel Estimation in Coherent Optical OFDM Systems

Xiaojie Wang, Benedikt Leible, Wenhao Wang, David Rörich, and Stephan ten Brink

Institute of Telecommunications, Pfaffenwaldring 47,

University of Stuttgart, 70569 Stuttgart, Germany

Email: {xwang, benedikt.leible, wenhao.wang, roerich, tenbrink}@inue.uni-stuttgart.de

Abstract—Coherent optical orthogonal frequency division multiplexing (CO-OFDM) is considered to be promising technique for meeting the ever increasing demand of data rate. It exhibits many advantages of coherent detection and OFDM, making the optical transmission over fiber extremely robust against distortions such as chromatic dispersion and polarisation mode dispersion. However, CO-OFDM is sensitive to IQ imbalance, in particular, when a homodyne (or direct down-conversion) receiver is used. In this paper, we study the impact of transmitter and receiver side IQ imbalance on coherent optical transmission over a single-mode fiber. Moreover, we investigate different methods, particularly in the frequency domain, to jointly compensate the IQ imbalance and to equalize the optical fiber channel, taking the effect of chromatic dispersion into account. The proposed minimum mean square error (MMSE) compensation algorithm shows superior performance, compared to conventional method. Furthermore, an optimum design of training sequence is derived and expressed in a closed-form, which provides significant performance gains even without applying IQ imbalance compensation.

I. INTRODUCTION

Coherent optical orthogonal frequency division multiplexing (CO-OFDM) has been shown to be a promising technology for robust transmission over optical fiber, since chromatic dispersion (CD) and polarisation mode dispersion (PMD) can be effectively compensated in the electrical domain using digital signal processing (DSP) [1], [2]. Furthermore, it enables scalability to the ever increasing demand of data rate and adaptability to reconfigurable optical networks. OFDM relies on the orthogonality of its subcarriers, thus it is very sensitive to any non-linearity which destroys the orthogonality between subcarriers. Therefore, nonlinearity caused by hardware imperfections should be compensated, preferably in the electrical domain since optical signal processing is expensive and usually more demanding.

A well-known transmitter (IQ modulator) and receiver (2×4 90° Hybrid) hardware imperfections is IQ imbalance. Ideally, the inphase and quadrature branches constitute an orthonormal basis in the complex plane. However, phase and amplitude error are introduced by hardware imperfection. Due to the phase error, the I-branch is not perpendicular to the Q-branch, which results in cross-talk between the two branches. An amplitude error means that I- and Q-axes are differently scaled. In single carrier (SC) systems, amplitude imbalance alone does not cause any crosstalk, since I- and Q-branch are orthogonal to each other in the absence of phase imbalance. However, the minimum Euclidean distance of the constellation

is reduced leading to a degradation of system performance. In contrast, amplitude imbalance alone destroys the orthogonality between OFDM subcarriers resulting in crosstalk, or intercarrier interference (ICI) [3].

IQ imbalance is considered a critical performance limiting impairment, particularly for homodyne receivers. Since homodyne receiver is today's most popular technique to save hardware costs, impairments caused by IQ imbalance have to be mitigated. The impact of IQ imbalance and its compensation are studied in [4] in terms of bit error rate. In [5], a theoretical analysis of symbol error rate in the presence of IQ imbalance is presented considering wireless fading channels. Many experimental results are reported for the compensation of IQ imbalance in CO-OFDM in [6] and [7], mostly using time domain algorithms. However, to the best knowledge of the authors, the optimum estimation and equalization of IQ imbalance with an optimal training sequence design have not been yet presented.

In this paper, we address the IQ imbalance problem at both the optical transmitter and receiver, taking the chromatic dispersion of the fiber into account. The impact of IQ imbalance is thoroughly analyzed in general and then further elaborated for the fiber-optical channel. The one-tap equalizer at the OFDM receiver, which is used for frequency domain equalization, is extended to compensate both transmit and receive IQ imbalance. The contributions of this paper are 1) a systematical analysis of the impact of IQ imbalance with and without perfect channel knowledge; 2) we find the optimum OFDM pilot symbols (or preamble) to improve the joint compensation of chromatic dispersion and IQ imbalance; 3) an optimum estimation and equalization algorithm in the sense of minimum mean square error (MMSE) is presented.

II. CO-OFDM WITH TX AND RX IQ IMBALANCE

In Fig. 1, we show the system model of CO-OFDM [8]. An optical IQ modulator consists of two Mach-Zehnder-Modulators (MZM) in push-pull (AM) mode, which modulate the I- and Q-signal based on the light emitted by a laser diode (LD). The effect of amplitude imbalance is modeled as asymmetrically split power into I- and Q-branch, denoted by $a_{I,tx}^2$ and $a_{Q,tx}^2$, respectively. The phase imbalance is modeled as an additional phase shift of ϕ_{tx} at the Q-branch, which causes interference to the inphase signal component. At the receiver front-end (Hybrid), phase imbalance ϕ_{rx} and

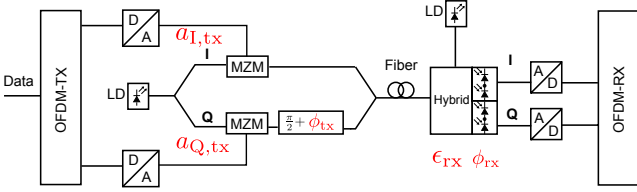


Figure 1. System model of CO-OFDM with Tx and Rx IQ imbalance

amplitude imbalance $\epsilon_{rx} = 20 \log(\frac{a_{I,rx}}{a_{Q,rx}})$ are also present. It can be shown that, provided the length of the cyclic prefix (CP) is longer than the channel impulse response (CIR), the received signal at subcarrier n can be expressed as [4]

$$R_n = \alpha_{tx}^* \beta_{rx}^* S_{-n}^* H_{-n}^* + \beta_{rx}^* \beta_{tx} S_n H_{-n}^* + \alpha_{rx} \alpha_{tx} S_n H_n + \alpha_{rx} \beta_{tx}^* S_{-n}^* H_n + N_n, \quad (1)$$

where

- S_n and S_{-n} denote the modulated symbols, e.g. QAM symbols, at subcarrier n and $-n$, respectively
- H_n and H_{-n} represent the discrete-frequency channel transfer function (CTF) of the optical fiber at subcarriers n and $-n$, respectively
- N_n denotes the amplified spontaneous emission (ASE) noise, which follows a Gaussian distribution with zero mean and variance σ^2
- $\alpha_{tx} = \frac{a_{I,tx} + a_{Q,tx}}{2} e^{j\phi_{tx}}$ and $\beta_{tx} = \frac{a_{I,tx} - a_{Q,tx}}{2} e^{-j\phi_{tx}}$ are other representations of the IQ imbalance at the IQ modulator
- similar to α_{tx} and β_{tx} , the constants α_{rx} and β_{rx} denote the IQ imbalance at receiver

Throughout this paper, we normalize the total power of I- and Q-branches, i.e., $a_{I,tx}^2 + a_{Q,tx}^2 = a_{I,rx}^2 + a_{Q,rx}^2 = 1$. Hence, the amplitude imbalance can be characterized by $\epsilon_{tx} = 20 \log(\frac{a_{I,tx}}{a_{Q,tx}})$ and, similarly, ϵ_{rx} .

Based on the analysis in (1), we show the impact of IQ imbalance on channel estimation and OFDM data symbols in the following. Assume that the channel coefficients are perfectly estimated, then the OFDM one-tap equalizer performs equalization, and the estimated data symbol at subcarriers n is thus obtained as

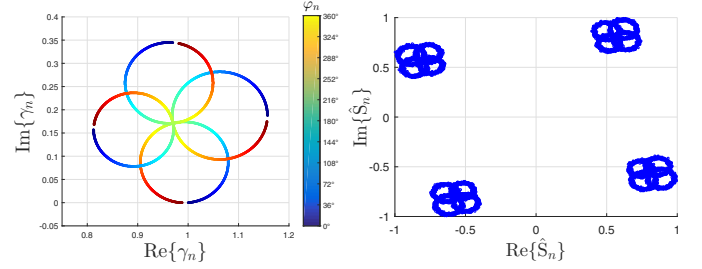
$$\hat{S}_n = \frac{R_n}{H_n} = \gamma_n \cdot S_n + \tilde{N}_n, \quad (2)$$

where γ_n is a complex scaling factor due to IQ imbalance, which can be expressed by

$$\gamma_n = c_n + r_n \frac{H_{-n}^*}{H_n} e^{j\varphi_n} \quad (3)$$

with $c_n = \alpha_{rx} \alpha_{tx} + \alpha_{rx} \beta_{tx}^* \frac{S_{-n}^*}{S_n}$ and $r_n = \beta_{rx}^* \beta_{tx} + \beta_{rx}^* \alpha_{tx}^* \frac{S_{-n}^*}{S_n}$. Moreover, since we assume that the fiber only exhibits CD, the term $\frac{H_{-n}^*}{H_n}$ solely leads to a phase shift $e^{j\varphi_n}$. Therefore, the scaling factor γ_n caused by IQ imbalance forms a circle in the complex plane with center point c_n and radius $|r_n|$. Depending on the applied signaling QAM-format, there exist

different possible values for c_n and r_n , thus it results in a different number of circles in the constellation diagram. In Fig. 2, the constellation diagram of the received signal \hat{S}_n of (2) and the scaling factor γ_n of (3) are shown. QPSK symbols S_n are transmitted on every subcarrier; the underlying SNR is set to 20 dB. The phase imbalance is set to, e.g., $\phi_{tx} = \phi_{rx} = 10^\circ$ and amplitude imbalance is neglected for the moment, i.e., $\epsilon_{tx} = \epsilon_{rx} = 0$ dB. Furthermore, the fiber length is chosen to be sufficiently long to observe a wide range of phase differences φ_n . For QPSK, the complex scaling factor induced by IQ



(a) Complex scaling factor γ_n (b) QPSK constellation corrupted by IQ imbalance, SNR = 20 dB

Figure 2. Impact of IQ imbalance with perfect channel knowledge

imbalance forms four circles in the complex plane, leading to translations and rotations of each data points S_n . Obviously, IQ imbalance introduces ICI. This substantially degrades the system performance.

Not only data symbols suffer from IQ imbalance, but also pilot symbols (used for channel estimation). Using (1) - (3), we obtain the channel estimates at subcarriers n as

$$\hat{H}_n = \frac{R_{n,p}}{S_{n,p}} = \gamma_{n,p} \cdot H_n + \tilde{N}_{n,p}, \quad (4)$$

where the subscript p indicates pilot symbols. In Fig. 3, the real and imaginary parts of the channel coefficients H_n and its estimates \hat{H}_n are shown for all subcarriers. The channel coefficients H_n are obtained for a fiber length of 80 km with a chromatic dispersion coefficient of $D_c = 17$ ps/km/nm. The estimates \hat{H}_n differ from the ideal value depending on the factor $\frac{S_{-n,p}^*}{S_{n,p}}$ which signifies the influence of the chosen pilot symbols on the estimation \hat{H}_n . For the channel estimation, a repetition preamble, consisting of N_T identical OFDM pilot symbols, is adopted. Using multiple pilot symbols helps to reduce the ASE noise variance by taking the average over N_T estimations. With the repetition preamble, the scaling factor $\gamma_{n,p}$ remains constant for every pilot symbol. The repetition preamble thus cannot benefit from averaging over multiple estimates in terms of reducing the error introduced by IQ imbalance. In order to obtain channel estimates that are less sensitive to IQ imbalance, a random preamble consisting of multiple randomly chosen pilots may be a better option. The random preamble benefits from the fact that the complex scaling factors for the transmitted pilot symbols are in general not identical for different values of $\frac{S_{-n,p}^*}{S_{n,p}}$ and tend to partially neutralize each other. The design of the preamble and its

impact on system performance will be discussed later in Sec. III-C and Sec. IV.

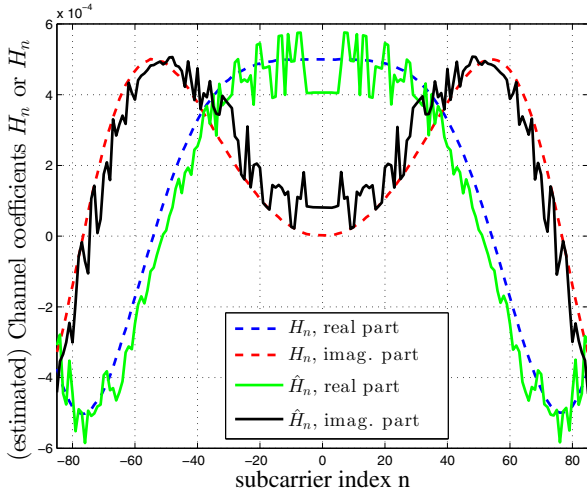


Figure 3. Impact of IQ imbalance on channel estimation

Usually, the erroneous channel estimates of (4), i.e., corrupted by noise and IQ imbalance, are used for the equalization. With (2), the signal at the receiver side after equalization using the distorted channel estimates can be described by

$$\hat{S}_n = \frac{R_n}{\hat{H}_n} = \frac{\gamma_n \cdot S_n H_n + \tilde{N}_n}{\gamma_{n,p} \cdot H_n + \tilde{N}_{n,p}} \approx \tilde{\gamma}_n S_n + \tilde{\tilde{N}}_n, \quad (5)$$

where $\tilde{\gamma}_n = \frac{\gamma_n}{\gamma_{n,p}}$ is a complex scaling factor, $\tilde{\tilde{N}}_n$ denotes the noise after equalization; we assume $\tilde{N}_{n,p}$ to be negligible since N_T pilot symbols are used. It can be seen that the

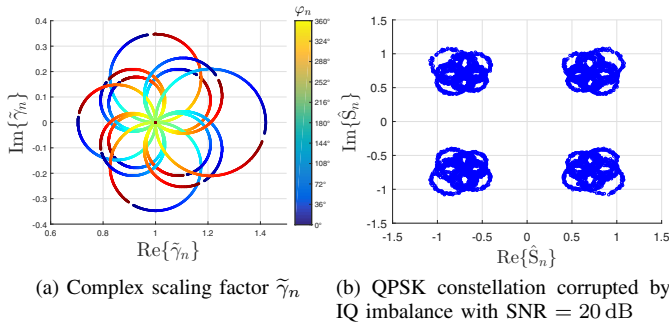


Figure 4. Impact of IQ imbalance with erroneous channel knowledge

two complex scaling factors γ_n and $\gamma_{n,p}$ both affect the estimated OFDM symbol at each subcarrier. Since the parameters α_{tx} , α_{rx} , β_{tx} , β_{rx} are assumed to be constant during the entire transmission process, the influence of the scaling factors is dependent on the expressions $\frac{S_n^*}{S_n}$, $\frac{S_{n,p}^*}{S_{n,p}}$ and $e^{j\varphi_n}$. In Fig. 4a, the complex scaling factor $\tilde{\gamma}_n$ considering IQ imbalance and erroneous channel estimates is plotted for QPSK modulation. Since $\frac{S_n^*}{S_n}$ and $\frac{S_{n,p}^*}{S_{n,p}}$ can each take on four different values for QPSK, the evaluation of the combined scaling factor can

be separated into 16 cases. There exist 4 trivial cases for which $\frac{S_n^*}{S_n} = \frac{S_{n,p}^*}{S_{n,p}}$ and the influence of IQ imbalance is successfully canceled out, i.e., $\tilde{\gamma}_n = \frac{\gamma_n}{\gamma_{n,p}} = 1$. The remaining 12 cases form circles in the complex plane. Since the number of possible cases increases for higher order QAM modulation schemes, the number of visible circles in the complex plane would also increase. Furthermore, the combined scaling factor can affect every constellation point. This leads to rotations and translations of the constellation diagram for every signal point, as shown in Fig. 4b.

III. CHANNEL EQUALIZATION AND IQ IMBALANCE COMPENSATION

In general, IQ imbalance destroys the orthonormal properties of the I/Q channels, inducing interference between every OFDM subcarrier-pair in the transmitted signals or/and received signals. Since the core principle of OFDM is orthogonality between subcarriers, it is essential to compensate this impairment. Mathematically, the effect of IQ imbalance is actually a transformation of axes. Unless one axis is fully masked out, e.g., $a_{Q,rx} = 0$ or $\phi_{tx} = \frac{\pi}{2}$, this effect is reversible and can be mitigated using inverse transformation. There exist already several algorithms to compensate IQ imbalance, e.g. in [4], [7]. Due to the nature of OFDM, we restrict ourselves to frequency domain approaches, which was presented in [4]. In this section, we briefly review the Least-Squares compensation approach. Then, we extend this approach to an optimal minimum mean square error (MMSE) compensation, considering additionally the noise statistics. At last, an optimum design of training sequences for the compensation is presented.

The transmitted data frame is divided into two parts: preamble and payload, as depicted in Fig. 5. The preamble consists of N_T training OFDM symbols or pilot symbols, which are used to estimate the CTFs \hat{H}_n . The estimated channel coefficients are then applied to recover the transmitted data symbols at the corresponding subcarriers. In the presence of

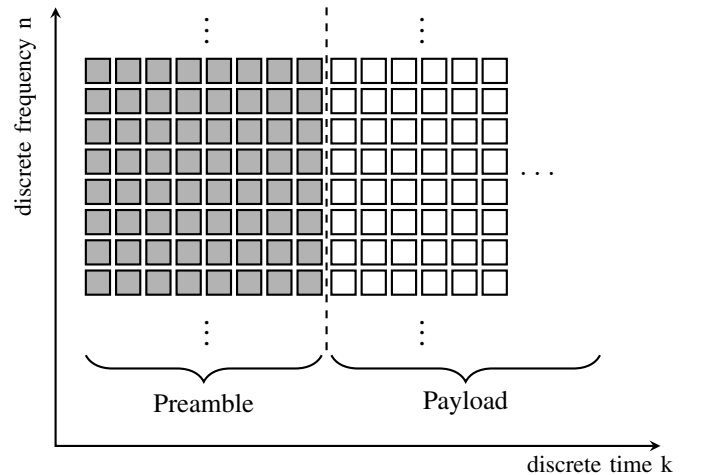


Figure 5. Frame structure

IQ imbalance at transmitter and receiver, the one-tap equalizer

of OFDM first performs estimation of the channel and IQ imbalance coefficients jointly, and subsequently mitigates the impact of IQ imbalance and chromatic dispersion of the fiber to recover the transmitted data symbols.

A. Least-Squares Estimation and Compensation

According to (1), the received signal at the n -th subcarrier is solely interfered by the $-n$ -th subcarrier. Hence, we stack the two signals into a vector and express it in matrix form as

$$\underbrace{\begin{bmatrix} R_n \\ R_{-n}^* \end{bmatrix}}_{\mathbf{r}_n} = \underbrace{\begin{bmatrix} \tilde{H}_{1,n} & \tilde{H}_{3,n} \\ \tilde{H}_{2,n} & \tilde{H}_{4,n} \end{bmatrix}}_{\tilde{\mathbf{H}}_n} \cdot \underbrace{\begin{bmatrix} S_n \\ S_{-n}^* \end{bmatrix}}_{\mathbf{s}_n} + \underbrace{\begin{bmatrix} N_n \\ N_{-n}^* \end{bmatrix}}_{\mathbf{n}_n}, \quad (6)$$

where

$$\tilde{\mathbf{H}}_n = \begin{bmatrix} \alpha_{\text{rx}}\alpha_{\text{tx}}H_n + \beta_{\text{rx}}^*\beta_{\text{tx}}H_{-n}^* & \alpha_{\text{tx}}^*\beta_{\text{rx}}^*H_{-n}^* + \alpha_{\text{rx}}\beta_{\text{tx}}^*H_n \\ \alpha_{\text{tx}}\beta_{\text{rx}}H_n + \alpha_{\text{rx}}^*\beta_{\text{tx}}H_{-n}^* & \alpha_{\text{rx}}^*\alpha_{\text{tx}}^*H_{-n}^* + \beta_{\text{rx}}\beta_{\text{tx}}^*H_n \end{bmatrix}$$

denotes the mixed channel and IQ imbalance coefficients. For the joint channel equalization and IQ imbalance compensation, it is necessary to estimate all the elements of $\tilde{\mathbf{H}}_n$. To estimate 4 coefficients, 2 OFDM pilot symbols are inevitable. Stacking two OFDM pilot symbols into a vector, the received pilot symbol vector is formulated as

$$\underbrace{\begin{bmatrix} \mathbf{r}_{1,n} \\ \mathbf{r}_{2,n} \end{bmatrix}}_{\mathbf{r}_{n,p}} = \underbrace{\begin{bmatrix} S_{1,n} & 0 & S_{1,-n}^* & 0 \\ 0 & S_{1,n} & 0 & S_{1,-n}^* \\ S_{2,n} & 0 & S_{2,-n}^* & 0 \\ 0 & S_{2,n} & 0 & S_{2,-n}^* \end{bmatrix}}_{\mathbf{S}_{n,p}} \underbrace{\begin{bmatrix} \tilde{H}_{1,n} \\ \tilde{H}_{2,n} \\ \tilde{H}_{3,n} \\ \tilde{H}_{4,n} \end{bmatrix}}_{\tilde{\mathbf{h}}_n} + \tilde{\mathbf{n}}_n, \quad (7)$$

where $\tilde{\mathbf{n}}_n = [\mathbf{n}_{1,n}, \mathbf{n}_{2,n}]$ denotes the noise vector composed of noise at subcarriers $\pm n$ of two consecutive pilot symbols. To estimate the parameters, $\mathbf{S}_{n,p}^{-1}$ is multiplied with the input vector $\mathbf{r}_{n,p}$ and then similarly $\tilde{\mathbf{H}}_n^{-1}$ is multiplied with \mathbf{r}_n to obtain the estimates of the data symbols.

B. MMSE Estimation and Compensation

In the estimation phase, the parameters $\tilde{\mathbf{H}}_n$ are constant. Thus, LS estimation is also optimal in the sense of minimum variance unbiased estimation (MVUE) [9]. If $N_T > 2$ training symbols are sent for more accurate parameter estimation, several matrix equations of (7) can be collected and the final parameter estimate is obtained by taking the average.

At the equalization stage, a more sophisticated method can be applied, i.e., the linear MMSE method, in which the noise statistics are also taken into account. With (6), the MMSE receive matrix can be written as

$$\mathbf{W}_{\text{mmse},n} = \left(\tilde{\mathbf{H}}_n^H \tilde{\mathbf{H}}_n + \mathbf{R}_{\text{nn}} \right)^{-1} \cdot \tilde{\mathbf{H}}_n^H, \quad (8)$$

where $\mathbf{R}_{\text{nn}} = \sigma^2 \cdot \begin{bmatrix} 1 & 2\alpha_{\text{rx}}\beta_{\text{rx}}^* \\ 2\alpha_{\text{rx}}^*\beta_{\text{rx}} & 1 \end{bmatrix}$ is the auto-covariance matrix of the received noise vector. The correlation between noise instances is introduced by IQ imbalance at the receiver frontend. The proof is shown in Appendix A. The correlation coefficients can be estimated using zero subcarriers (guard bands) in CO-OFDM systems.

C. Preamble design

According to (7), the parameter estimation is significantly affected by the choice of pilot sequence, i.e., the pilot matrix $\mathbf{S}_{n,p}$. In order to obtain accurate parameter estimates, we propose an optimum design of the preamble in the MMSE-sense to facilitate the aforementioned joint channel equalization and IQ imbalance compensation. The optimization problem is formulated as

$$\begin{aligned} \mathbf{S}_{n,p}^{\text{opt}} &= \arg \min_{\mathbf{S}_{n,p}} \|\mathbf{S}_{n,p}^{-1} \cdot \tilde{\mathbf{n}}_n\|^2 \\ \text{subject to } &\|S_{1,\pm n}\|^2 = \|S_{2,\pm n}\|^2 = 1. \end{aligned} \quad (9)$$

By doing this, the total noise power is minimized with the constraint of limited signal power at every subcarrier and pilot symbol. The minimum noise variance in (9) is reached if the condition

$$\arg S_{1,n}S_{2,-n}^* = -\arg S_{1,-n}^*S_{2,n} \quad (10)$$

is fulfilled. The proof is shown in the Appendix B.

IV. SIMULATION RESULTS

For numerical simulation, the total number of OFDM subcarriers is set to 256, sharing an available bandwidth of 32 GHz. Of those, 5 subcarriers around DC and 85 subcarriers at the edges are deactivated to serve as guard bands. The standard single mode fiber (SMF) has a length of 80 km with a chromatic dispersion coefficient of $D_c = 17$ ps/km/nm. The launch power of the laser diode is assumed to be sufficiently small so that the non-linearity of the fiber can be neglected. Further, the system operates at the wavelength of 1550 nm. To protect the received OFDM symbols from ISI, a cyclic prefix (CP) with a length of 8 samples is inserted. The frequencies of transmit and receive laser diode are assumed to be perfectly matched; the compensation of carrier frequency offset is considered in, e.g., [10].

From Sec. II we have seen that IQ imbalance induces interference from mirror frequencies. In Fig. 6 we show the impact of IQ imbalance on the bit error rate (BER) of the CO-OFDM system, applying different QAM constellations. The preamble for channel estimation consists of $N_T = 10$ identical pilot symbols, which will be referred to as repetition preamble. First of all, either only transmit side or receive side phase imbalance is present, i.e., $\phi_{\text{tx}} = \phi_{\text{rx}} = 10^\circ$. To achieve a target BER of 10^{-3} , an additional optical SNR (OSNR) of 0.6 dB and 3.7 dB is needed for QPSK and 16-QAM signaling with $\phi_{\text{rx}} = 10^\circ$, respectively, if IQ imbalance is not compensated. For higher order QAM modulations such as 64-QAM or 256-QAM, an error floor at BER 2% and 10% shows up for high OSNRs, respectively.

To jointly perform IQ imbalance compensation and channel equalization, LS and MMSE approaches can be employed. The two approaches differ only at the data equalization stage. At the training stage (preamble is transmitted), the parameters are obtained using the same method. For an optimum estimation, the optimal preamble is proposed in Sec. III-C. Besides this optimal preamble, we also introduce a random preamble

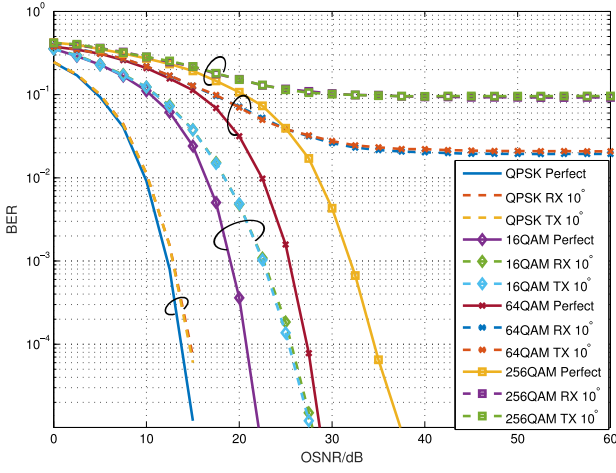
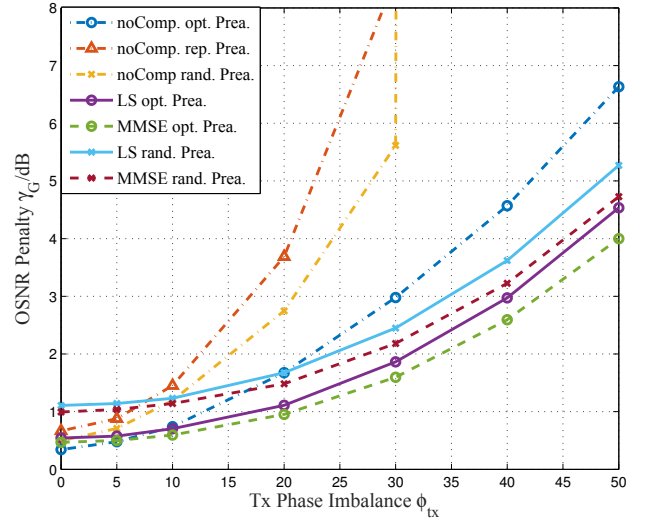


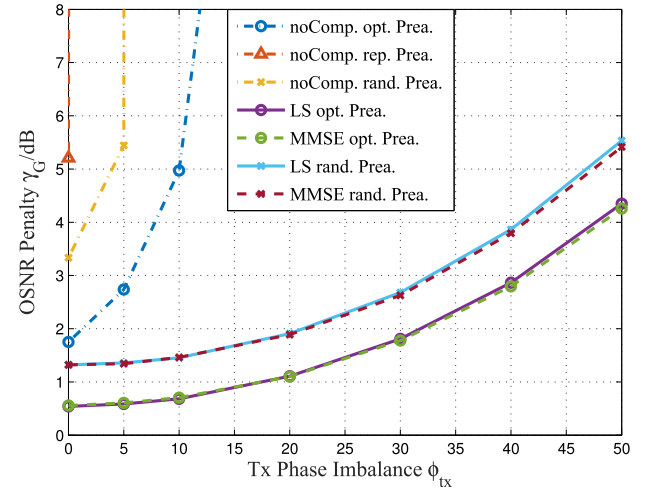
Figure 6. BER curves vs OSNR, without IQ imbalance compensation

for comparison purpose. The random preamble consists of randomly selected pilot symbols, which, however, allows the inversion of pilot matrices $S_{n,p}$, see (7), to jointly estimate IQ imbalance and channel coefficients. Moreover, the auto-covariance matrix of noise for MMSE-equalization is also estimated at the training stage using the deactivated zero subcarriers. In Fig. 7, the performance of LS and MMSE approaches in combination with random and optimized preamble is compared in terms of OSNR penalty at a target BER of 10^{-3} . The OSNR penalty is defined as the additionally required OSNR compared to the case without any IQ imbalance. In this simulation, amplitude imbalance is also included, with $\epsilon_{tx} = \epsilon_{rx} = 1$ dB. Since the phase imbalance ϕ_{rx} at the receiver can be completely compensated, we show solely the results for different ϕ_{tx} , i.e., $\phi_{rx} = 0$. With the optimized preamble, the OSNR penalty is reduced by about 0.6 dB and by 0.78 dB for the LS approach with QPSK and 16-QAM compared to the case with random preamble, respectively. For higher order QAM (curves not shown), 1.38 dB and 3.94 dB gain can be achieved for 64-QAM and 256-QAM, respectively. Interestingly, the optimized preamble also provides significant OSNR gain even if IQ imbalance is not compensated. The reason for the gain is that the distortion of IQ imbalance is cancelled out when averaging over successive distorted channel estimates thanks to the well-designed pilot sequence. Furthermore, the proposed MMSE method outperforms the LS approach, especially for QPSK with large phase impairment. For higher order QAM, there is almost no gain, as high OSNR values are typically required for the target BER. However, the IQ imbalance compensation is essential for higher order QAM modulation formats. In Fig. 8, the performance of LS and MMSE compensation are compared in terms of error vector magnitude (EVM). As expected, the MMSE method outperforms the LS method particularly for low OSNRs ranging from 0 to 15 dB.

Finally, we show the influence of the number of pilot symbols on the quality of IQ imbalance compensation in Fig.



(a) QPSK with IQ imbalance, $\epsilon_{tx} = \epsilon_{rx} = 1$ dB and $\phi_{rx} = 0$



(b) 16-QAM with IQ imbalance, $\epsilon_{tx} = \epsilon_{rx} = 1$ dB and $\phi_{rx} = 0$

Figure 7. OSNR Penalty with MMSE and LS compensation and different types of preamble

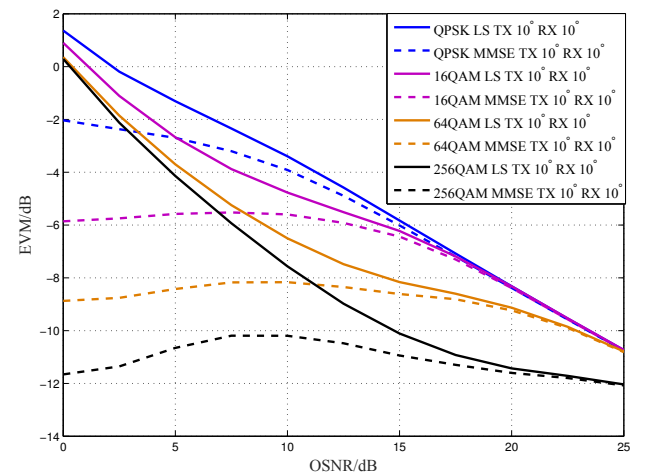


Figure 8. Comparison of estimated EVM between MMSE and LS approach

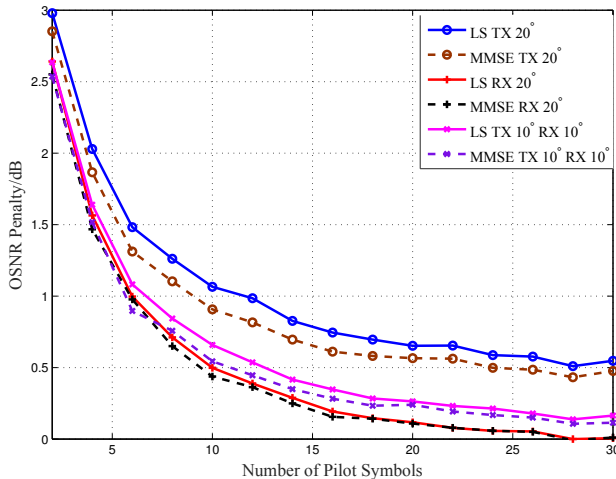


Figure 9. OSNR penalty vs number of pilot symbols with QPSK

9. If more pilot symbols are available for the joint estimation, the channel and IQ imbalance parameters can be estimated more precisely. Thus, the OSNR penalty is reduced. However, the OSNR penalty saturates with increasing number of pilots due to remaining noise and interference from the equalization. This result can be utilized to determine the minimum number of required pilots for a given target OSNR penalty.

V. CONCLUSIONS

This paper addresses the IQ imbalance problem in coherent optical OFDM systems considering the chromatic dispersion of single mode fiber. The impact of IQ imbalance at transmitter and receiver is thoroughly analyzed for cases with and without perfect channel knowledge. A systematic framework for the analysis of impact of IQ imbalance is built. Furthermore, different methods, i.e., LS and MMSE equalization for joint IQ imbalance compensation and channel estimation are presented. An optimum design of training sequences with power constraints is derived and we find the closed-form solution. Simulation results show that the MMSE equalization outperforms the LS approach in terms of error vector magnitude and OSNR penalty for a target BER of 10^{-3} . Moreover, the proposed optimum training sequence design significantly improves the system performance in the presence of IQ imbalance, even if compensation methods are not applied due to its optimized structure.

APPENDIX A

PROOF OF NOISE AUTOCOVARIANCE

Assume that solely noise \tilde{n} is the input of the receiver with IQ imbalance, characterized by the parameters α_{rx} and β_{rx} . The received noise is thus expressed as $n = \alpha_{\text{rx}}\tilde{n} + \beta_{\text{rx}}^*\tilde{n}^*$. After OFDM-FFT receiver, the frequency domain noise can be written as $N_n = \alpha_{\text{rx}}\tilde{N}_n + \beta_{\text{rx}}^*\tilde{N}_{-n}^*$. Thus, the noise vector \mathbf{n}_n is given by

$$\mathbf{n}_n = \begin{bmatrix} \alpha_{\text{rx}} & \beta_{\text{rx}}^* \\ \beta_{\text{rx}} & \alpha_{\text{rx}}^* \end{bmatrix} \cdot \begin{bmatrix} \tilde{N}_n \\ \tilde{N}_{-n}^* \end{bmatrix}$$

where \tilde{N}_n and \tilde{N}_{-n}^* are independently Gaussian distributed with variance σ^2 . Without loss of generality, the subindex n is dropped in the following. The auto-covariance matrix of \mathbf{n} is obtained by $\mathbf{R}_{\mathbf{nn}} = \text{E}[\mathbf{n}\mathbf{n}^H] = \sigma^2 \cdot \begin{bmatrix} 1 & 2\alpha_{\text{rx}}\beta_{\text{rx}}^* \\ 2\alpha_{\text{rx}}^*\beta_{\text{rx}} & 1 \end{bmatrix}$.

APPENDIX B

PROOF OF OPTIMUM PREAMBLE

We prove the condition in (10), which leads to a minimum total noise variance $\|\mathbf{S}_{n,p}^{-1} \cdot \tilde{\mathbf{n}}_n\|^2$. Apparently, the total noise power can be expressed as $J = \|\mathbf{S}_{n,p}^{-1} \cdot \tilde{\mathbf{n}}_n\|^2 = \text{tr}(\mathbf{S}_{n,p}^{-1} \tilde{\mathbf{n}}_n \tilde{\mathbf{n}}_n^H \mathbf{S}_{n,p}^{-1H}) = \sigma^2 \|\mathbf{S}_{n,p}^{-1}\|_{\text{F}}^2$, where $\text{tr}(\cdot)$ denotes the trace-operator and $\|\cdot\|_{\text{F}}^2$ denotes the Frobenius norm of a matrix. It is assumed that the noise is independent of each other, yielding $\text{E}[\tilde{\mathbf{n}}_n \tilde{\mathbf{n}}_n^H] = \sigma^2 \cdot \mathbf{I}$, with \mathbf{I} being the identity matrix. Since the matrix $\mathbf{S}_{n,p}$ has a very special structure, its inverse matrix exhibits a simple form

$$\mathbf{S}_{n,p}^{-1} = \frac{1}{D_p} \begin{bmatrix} S_{2,-n}^* & 0 & -S_{1,-n}^* & 0 \\ 0 & S_{2,-n}^* & 0 & -S_{1,-n}^* \\ -S_{2,n} & 0 & S_{1,n} & 0 \\ 0 & -S_{2,n} & 0 & S_{1,n} \end{bmatrix},$$

where $D_p = S_{1,n}S_{2,-n}^* - S_{1,-n}^*S_{2,n}$. With some mathematical manipulation, the total noise variance is $J = \frac{8}{\|D_p\|^2}$. The minimization problem transforms to a problem of maximizing $\|D_p\|^2$. With the triangle inequality for complex numbers, we obtain that $\|D_p\|^2 \leq \|S_{1,n}S_{2,-n}^*\|^2 + \|S_{1,-n}^*S_{2,n}\|^2$. The maximum is obtained, if (10) is fulfilled.

REFERENCES

- [1] W. Shieh and C. Athaudage, "Coherent optical orthogonal frequency division multiplexing," *Electronics Letters*, vol. 42, no. 10, pp. 587–589, May 2006.
- [2] F. Buchali, R. Dischler, and X. Liu, "Optical OFDM: A promising high-speed optical transport technology," *Bell Labs Technical Journal*, vol. 14, no. 1, pp. 125–146, Spring 2009.
- [3] C.-L. Liu, "Impacts of I/Q Imbalance on QPSK-OFDM-QAM Detection," in *International Conference on Consumer Electronics, ICCE. Digest of Technical Papers.*, June 1998, pp. 384–385.
- [4] A. Tarighat and A. H. Sayed, "Joint compensation of transmitter and receiver impairments in OFDM systems," *IEEE Transactions on Wireless Communications*, vol. 6, no. 1, pp. 240–247, Jan 2007.
- [5] M. Windisch and G. Fettweis, "Performance Degradation due to I/Q Imbalance in Multi-Carrier Direct Conversion Receivers: A Theoretical Analysis," in *2006 IEEE International Conference on Communications*, vol. 1, June 2006, pp. 257–262.
- [6] S. Chen, A. A. Amin, and W. Shieh, "Real-time IQ imbalance compensation for coherent optical OFDM transmission," in *Optical Fiber Communication Conference and Exposition (OFC/NFOEC) and the National Fiber Optic Engineers Conference*, March 2011, pp. 1–3.
- [7] H. S. Chung, S. H. Chang, and K. Kim, "Effect of IQ Mismatch Compensation in an Optical Coherent OFDM Receiver," *IEEE Photonics Technology Letters*, vol. 22, no. 5, pp. 308–310, March 2010.
- [8] D. Rörich, X. Wang, M. Bernhard, and J. Speidel, "Optimal Modulation Index of the Mach-Zehnder Modulator in a Coherent Optical OFDM System Employing Digital Predistortion," in *14. ITG Symposium Proceedings of Photonic Networks*, May 2013, pp. 1–6.
- [9] S. M. Kay, *Fundamentals of Statistical Signal Processing, Volume I: Estimation Theory*. New Jersey: Prentice-Hall, 1993.
- [10] D. Rörich, I. Vaklinov, and S. ten Brink, "Robust Carrier Frequency Offset Estimation with Reduced Overhead for Coherent Optical OFDM Systems," in *16. ITG Symposium Proceedings of Photonic Networks*, May 2015, pp. 1–7.